Influence of H_2 on the Gas-Phase Decomposition of Formic Acid: A Theoretical Study

Shao-Wen Hu,* Xiang-Yun Wang, Tai-Wei Chu, and Xin-Qi Liu

Department of Applied Chemistry, College of Chemistry and Molecular Engineering, Peking University, Beijing, China 100871

Received: April 15, 2005; In Final Form: August 13, 2005

Gas-phase decomposition of formic acid results in final products CO + H_2O and CO_2 + H_2. Experimentally, the CO/CO_2 ratio tends to be large, in contradiction with mechanism studies, which show almost equal activation energies for dehydration and decarboxylation. In this work, the influence of H_2 on the decomposition mechanism of HCOOH was explored using ab initio calculations at the CCSD(T)/6-311++G**//MP2/6-311++G** level. It was found that, in the presence of H_2, the reaction channels leading to CO + H_2O are more than those leading to CO_2 + H_2. With competitive energy, H_2 addition to HCOOH can reduce the latter into HCHO, which then dissociates into CO + H_2 catalyzed by H_2O. Compared to *trans*-HCOOH, *cis*-HCOOH and *cis*-$C(OH)_2$, conformers required for decarboxylation, are less populated due to interactions with H_2.

I. Introduction

Early experiments[1,2] show that gas-phase thermal decomposition of formic acid results in four final products: carbon dioxide and hydrogen from decarboxylation, HCOOH → CO_2 + H_2; carbon monoxide and water from dehydration, HCOOH → CO + H_2O. It is found that the CO/CO_2 ratio is as large as 10, implying that the decomposition favors the channel of dehydration. However, the activation energies of the two decomposition channels, estimated experimentally as well as calculated theoretically, did not indicate a significant difference to support such a mechanism.[3−5] To interpret the discrepancy, one of the dehydration products, water, has been suggested as a catalyst. Several theoretical investigations focus on the H_2O-catalyzed decomposition of HCOOH.[6−9] When water molecules are added to the system, however, the activation energies of decarboxylation and dehydration are both lowered. In some cases, decarboxylation, instead of dehydration, appears to be favored when more water molecules are involved. Therefore, the water-catalyzed mechanism can hardly interpret the domination of dehydration. On the other hand, one of the decarboxylation products, the hydrogen molecule, remains unexplored; yet, it may also play an important role in the decomposition of HCOOH. In the first place, as H_2 accumulates, interaction between HCOOH and H_2 may hinder further decomposition as indicated by an experimental study on water−gas shift reactions.[10] Second, H_2 may promote reduction of HCOOH to formaldehyde, which then dissociates into CO and H_2O. There are also some evidences showing that HCHO is present as one of the products of HCOOH decomposition catalyzed by certain metals.[11,12] To interpret these phenomena and the large CO/CO_2 ratio, this work intends to investigate the decomposition of formic acid by taking the hydrogen molecule into account.

II. Calculation Method

The geometry structures were fully optimized at the MP2 = Full/6-311++G**level. Transition states were located using synchronous transit-guided quasi-Newton (STQN) methods[13] in combination with stepwise partial optimization along each pathway with one geometric parameter fixed as constant. Frequency calculations were performed following each optimization to obtain the zero-point energy (ZPE) and to characterize all the stationary points located on the potential energy surface. Intrinsic reaction coordinate (IRC) calculations were performed to confirm the relationship of each transition state with its reactant and product. Single-point calculations at the CCSD(T) = Full/6-311++G**levels were performed to determine the electronic energies. The relative energies reported in the discussion and showed in the figures of pathways are obtained at the CCSD(T) = Full/6-311++G** level with MP2 = Full/6-311++G** calculated ZPE corrections. The Gaussian 98 program package[14] was employed for these calculations.

III. Results and Discussions

Energies calculated at two different theoretical levels are listed together with dipole moments and rotational constants for all the species in the Supporting Information, Table 1. Generally, relative energies calculated at the MP2/6-311++G** level are quite close to those calculated at the CCSD(T)/6-311++G** level. The same theoretical method has been used for the CO−H_2O system[15] and is comparable with results obtained by others.[4,5]

Each minimum structure on the potential energy surface was given a number. The symbol "TS" was added to specify transition state.

The geometry structure and relative energy of each species are shown in Figures 1−12. Reaction pathways with relative energy lower than 80 kcal/mol are summarized schematically in Figure 13. As a comparison, decomposition pathways of free HCOOH are shown in Figure 14.

III.A. HCOOH−H_2 Complexes. Eleven HCOOH−H_2 complexes were located as minima on the potential energy surface (Figure 1). Six of the them are *trans*-HCOOH associated with H_2, and the other five are *cis*-HCOOH associated with H_2.The largest binding energy between HCOOH and H_2 is −0.76 kcal/mol. The energy of the *cis*-HCOOH conformer is about 4 kcal/mol higher than that of the trans one. This value does not change as a H_2 molecule weakly associates with HCOOH. In HCOOH−H_2 (**1**) and HCOOH−H_2 (**2**), carboxyl hydrogen of HCOOH

* Corresponding author. E-mail: sw-hu@163.com.

10.1021/jp051973u CCC: $30.25
Published on Web 09/20/2005

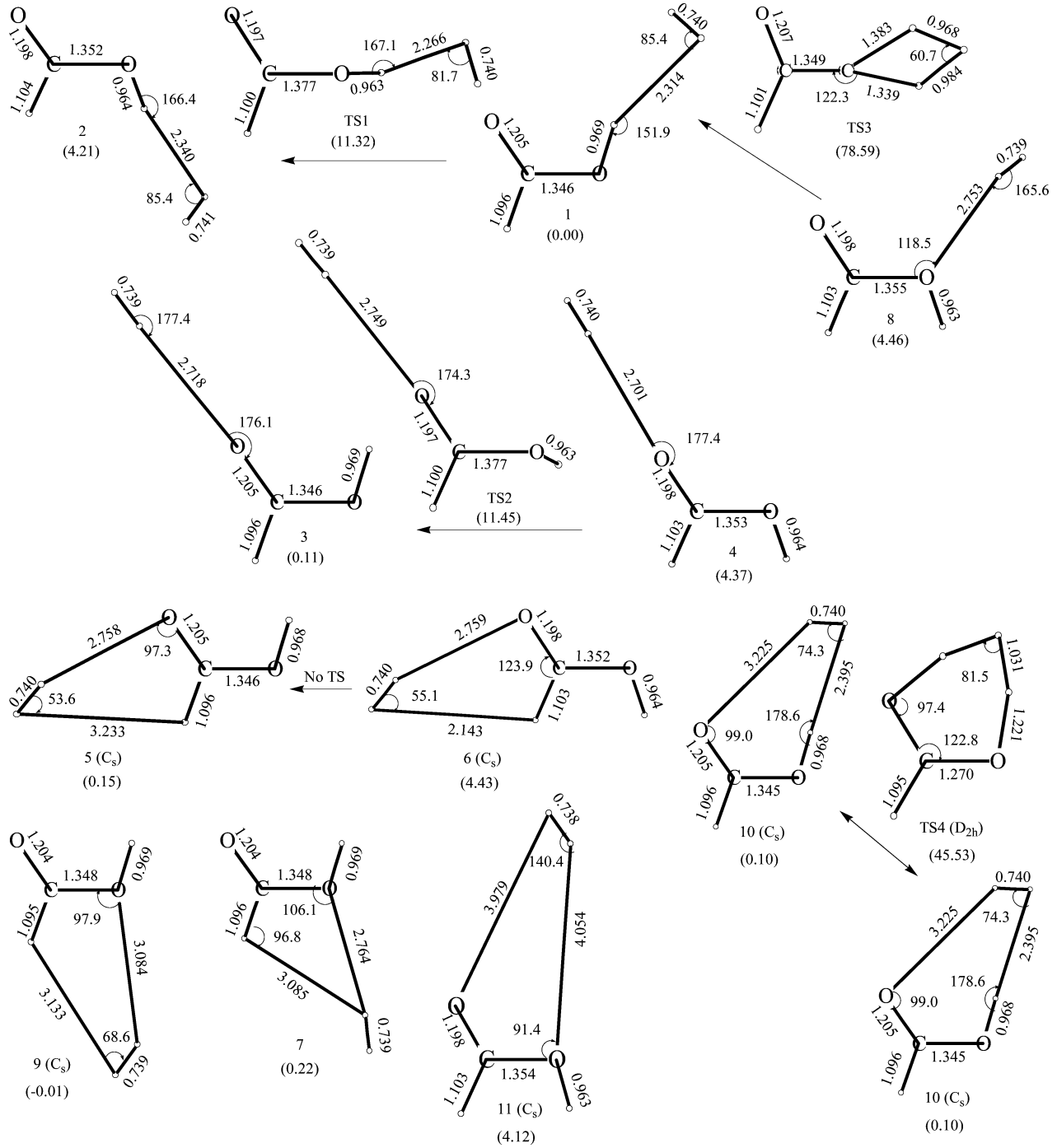

Figure 1. $HCOOH-H_2$ complexes and transition states for trans−cis conversion; bond lengths are in Å; angles are in degrees; the species beside the arrows are transition states; in parentheses, the symmetry (except for C_1) and relative energy (in kcal/mol) of each species are indicated.

bonds to the center of H_2. In $HCOOH-H_2$ (**3**) and $HCOOH-H_2$ (**4**), the carbonyl oxygen of HCOOH bonds to one H atom of H_2. The barriers of cis−trans conversion for these two pairs of conformers are about 11 kcal/mol, essentially the same as the value for free HCOOH, indicating that H_2 attachment dose not influence C−OH single-bond rotation in these species, as can be seen in transition states TS1 and TS2. The interconversion between *trans*-$HCOOH-H_2$ (**5**) and *cis*-$HCOOH-H_2$ (**6**), however, seems not as easy. No transition states connecting **5** and **6** were located despite extensive searching. Perhaps the bonding type between carbonyl oxygen and H_2, appearing in **5** and **6**, depends on electron conjugation of the O−C−O bond, which somewhat hinders the C−OH bond rotation. For similar reasons, no transition states connecting $HCOOH-H_2$ (**7**) and $HCOOH-H_2$ (**8**) were located. Instead, a transition state TS3 connecting **1** and **8** was located. Three H atoms are involved in forming a four-membered ring structure of TS3. Such a structure makes the barrier of the cis−trans conversion as high as 78.59 kcal/mol relative to that of **1**. There are still two more trans conformers, $HCOOH-H_2$ (**9**) and $HCOOH-H_2$ (**10**), and a cis one $HCOOH-H_2$ (**11**). The cis or trans counterparts of them do not exist because of specific orientation of HCOOH and H_2.

It is known that producing CO_2 and H_2 requires formation of *cis*-HCOOH. Free *trans*-HCOOH, with lower energy, is statistically more popular than the cis one. In the presence of the weakly bonded H_2, the trans−cis conversion of HCOOH is somewhat hindered. This may be one of the reasons that accounts for the large CO/CO_2 ratio.

Another feature is worth mentioning. For *trans*-HCOOH, hydrogen transfers from carboxyl oxygen to carbonyl oxygen

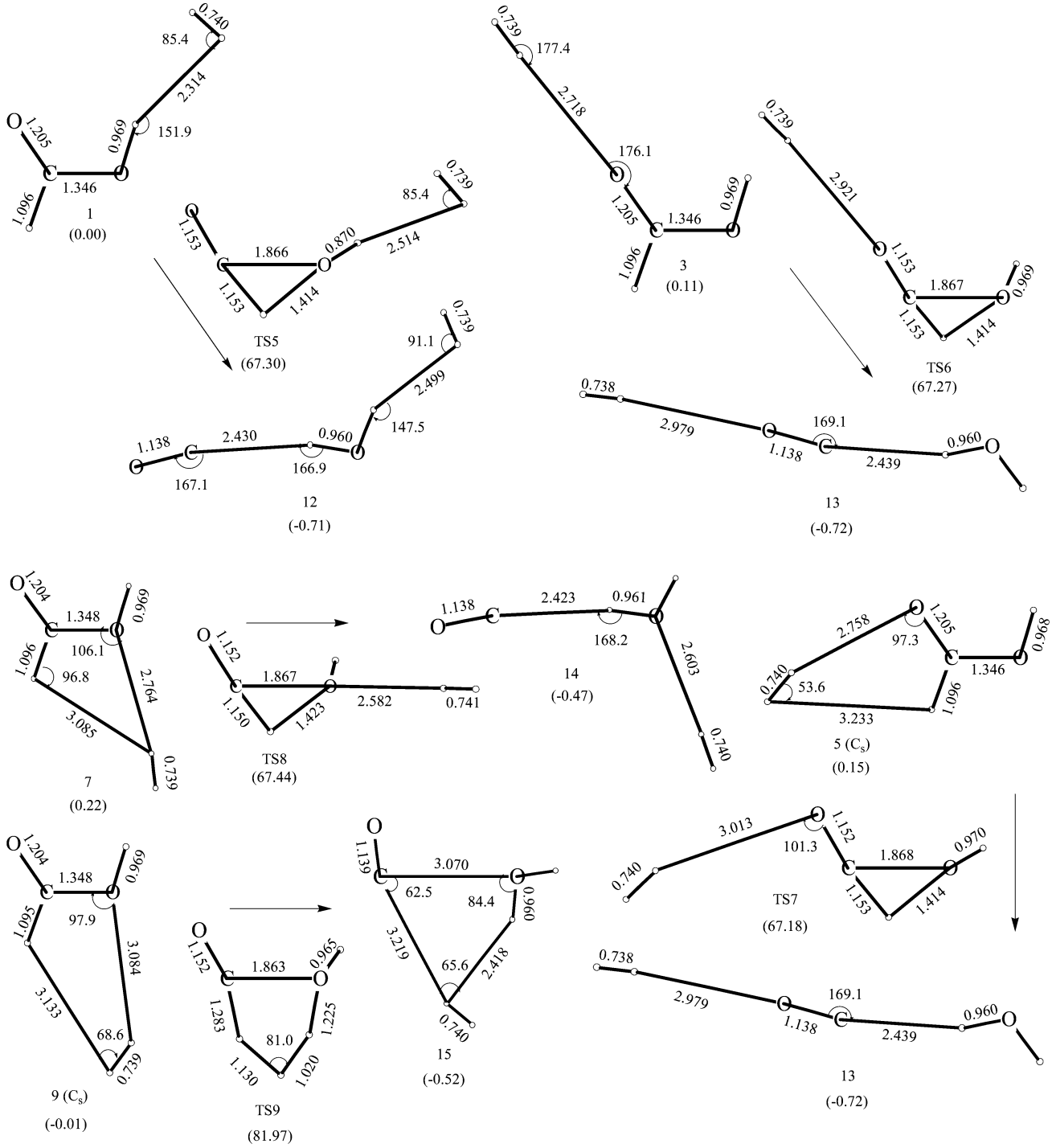

Figure 2. Species involved in pathways from HCOOH−H_2 to CO−H_2O−H_2; bond lengths are in Å; angles are in degrees; the species beside the arrows are transition states; in parentheses, the symmetry (except for C_1) and relative energy (in kcal/mol) of each species are indicated.

over an energy barrier of 35.38 kcal/mol.[16] The structure of the transition state shows D_{2h} symmetry with the H mediating between the two oxygen atoms. Such a transition state cannot be located for HCOOH−H_2 complexes. Instead, a symmetric transition state, TS4, was located. H transfers between the two oxygen atoms via a six-membered ring structure involving three H atoms, connecting the two same conformers **10**. The barrier is 45.53 kcal/mol relative to that of **1**. Therefore, the presence of H_2 also slows down the H transfer rate between the two oxygen atoms.

III.B. Dehydration and Decarboxylation of HCOOH. Four of the six trans HCOOH−H_2 conformers, **1**, **3**, **5**, and **7**, dissociate directly to CO and H_2O via H transfer from carbon to carboxyl oxygen (Figure 2). Starting from these conformers, dehydration is essentially not influenced by the H_2 molecule, as can be seen from four similar transition states TS5, TS6, TS7, and TS8. The only difference between the structures of these transition states is the position of the weakly attached H_2, which also determines the different interacting structures of the dissociated products, CO, H_2O, and H_2, as can be seen in CO−H_2O−H_2 (**12**), CO−H_2O−H_2 (**13**), and CO−H_2O−H_2 (**14**). The barrier heights are from 67.18 to 67.44 kcal/mol, essentially the same as the 67.24 kcal/mol required for dehydration of free HCOOH (Figure 14). Starting from **9**, H_2 takes part in the dehydration via a five-membered ring structure involving three H atoms (TS9), resulting in CO−H_2O−H_2 (**15**), another weakly

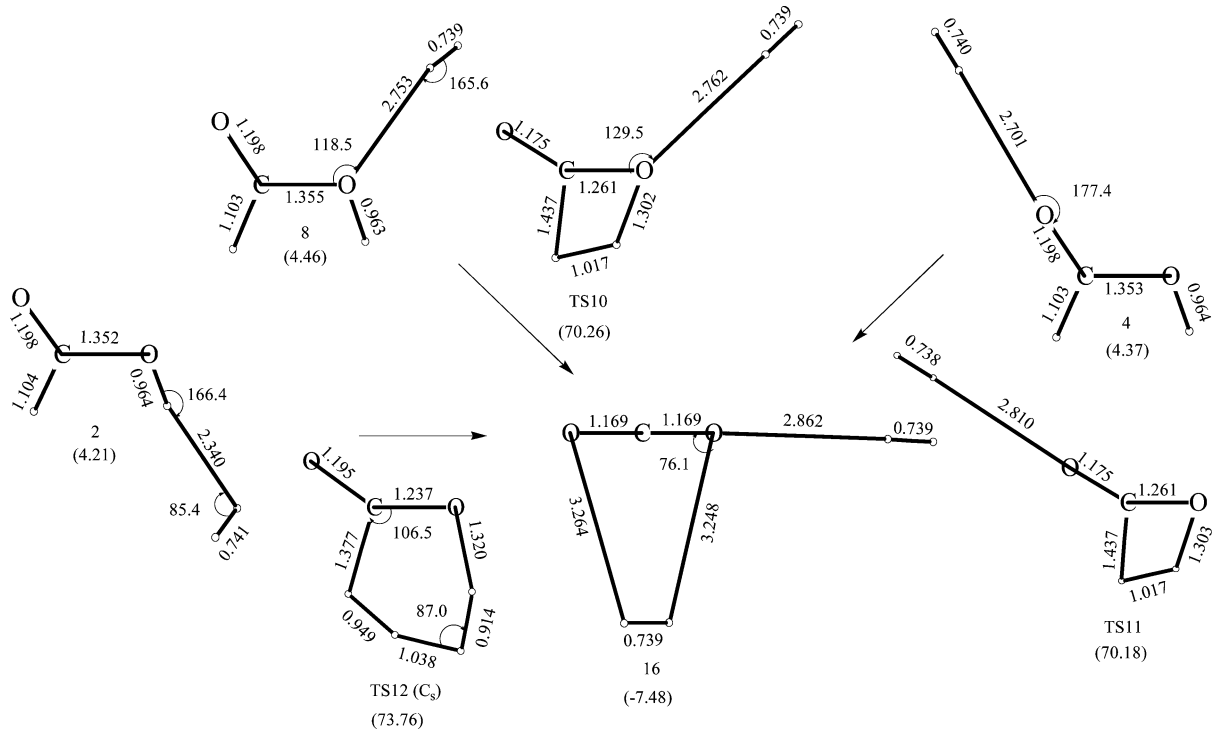

Figure 3. Species involved in pathways from HCOOH−H_2 to H_2−CO_2−H_2; bond lengths are in Å; angles are in degrees; the species beside the arrows are transition states; in parentheses, the symmetry (except for C_1) and relative energy (in kcal/mol) of each species are indicated.

associated trimolecular complex. The barrier for the process is 81.97 kcal/mol relative to that of **1**, about 15 kcal/mol higher than that for dehydration of free HCOOH. In this case, the presence of H_2 may also slow the dehydration of HCOOH.

Starting from cis HCOOH−H_2 complexes **2, 4**, and **8**, decarboxylation can proceed via three transition states, resulting in H_2−CO_2−H_2 (**16**) (Figure 3). In TS10 or TS11, H_2 bonds weakly to carbonyl or carboxyl oxygen. The barrier heights are 70.18 or 70.26 kcal/mol relative to that of **1**. Compared to the value of 81.66 kcal/mol for free HCOOH (Figure 14), it is quite remarkable that such weak interactions can lower the barriers about 11 kcal/mol. In another transition state, TS12, connecting **2** and **16**, a six-membered ring structure containing four H atoms is formed. The barrier is 73.76 kcal/mol relative to that of **1**.

In summary, the influence of H_2 on the activation energy of direct dehydration and decarboxylation is not significant. However, because the trans HCOOH−H_2 complex has more conformers than the cis one, and in some cases, trans−cis conversion is not as easy as in free HCOOH, the probability for dehydration may be larger than that of decarboxylation.

III.C. Pathways via Formation of $C(OH)_2$. In our previous work,[15] we found that dihydroxycarbene $C(OH)_2$ is an important intermediate connecting CO−H_2O, HCOOH, and CO_2−H_2. From free HCOOH, $C(OH)_2$ forms as H migrates from carbon to carbonyl oxygen. The barrier is about 75 kcal/mol (Figure 14). The energy values of various $C(OH)_2$ conformers range from 40 to 50 kcal/mol relative to that of HCOOH. In the presence of H_2, 6 of the 11 HCOOH−H_2 complexes, **1**, **2**, **3**, **4**, **5**, and **6**, can convert to 5 $C(OH)_2$−H_2 complexes **17**, **18**, **19**, **20**, and **21** via H migration from carbon to carbonyl oxygen (Figure 4). Six transition states TS13, TS14, TS15, TS16, TS17, and TS18 are energetically close (from 75.81 to 76.44 kcal/mol relative to **1**); their structures differ from each other by orientation of the OH group as well as the position of the weakly bonded H_2. Besides, four more $C(OH)_2$−H_2 complexes **22**, **23**, **24**, and **25**, with specific conformer of $C(OH)_2$ and position of H_2, cannot be produced directly by any of the HCOOH−H_2 complexes. Starting from **5** and **6**, two more transition states TS19 and TS20 exist, in which H transfers from C to O via a five-membered ring formed by a bond involving three H atoms. In these cases, because the energies of TS19 and TS20 are similar to those of TS17 and TS18, the concentration or partial pressure of H_2 rather than the temperature of the system may determine the probability of each reaction channel.

For free $C(OH)_2$, different conformers can convert to each other via single-bond rotation. The barriers are less than 19 kcal/mol. As a result of interacting with H_2, not all $C(OH)_2$−H_2 conformers can rotate their O−H bond over the small barrier. Only **17**, **18**, **21**, and **22**, with H_2 bonded weakly to hydroxyl hydrogen, can interconvert to each other in this way, as shown by TS21 and TS22, connecting **17** and **21** with **18**; TS23 and TS24, connecting **17** and **21** with **22** (Figure 5). The barriers range from 15 to 18 kcal/mol. Complexes **19**, **20**, **23**, **24**, and **25**, with H_2 bonded weakly to hydroxyl oxygen, can hardly interconvert with the other conformers. Only one transition state, TS25, was located between **17** and **20**. Instead of single-bond rotation, H transfers via a four-membered ring structure involving three H atoms. The much higher barrier of 117.55 kcal/mol relative to that of **1** makes the probability of the conversion very small. Likewise, a similar transition state, TS26, connecting **21** and **22** also exists, with an energy as high as 120.45 kcal/mol. Therefore, the conversion between **21** and **22** proceeds via the much lower transition state TS24.

Over barriers of about 76 kcal/mol relative to that of HCOOH, the transient intermediate $C(OH)_2$ can dissociate into CO and H_2O via dehydration (Figure 14). In the presence of H_2, similarly, $C(OH)_2$−H_2 complexes **19**, **21**, and **23** can dissociate into CO−H_2O−H_2 (**26**), CO−H_2O−H_2 (**27**), and CO−H_2O−H_2 (**28**), respectively (Figure 6). The transition states TS27, TS28, and TS29 are similar in energy (74.33, 74.17, and 74.24 kcal/mol relative to that of **1**) and different in relative positions of the weakly bonded H_2. Starting from **17**, dehydration can proceed via a six-membered ring structure involving a triangular H−H−H bond (TS30), resulting in **28**. The higher barrier (95.70

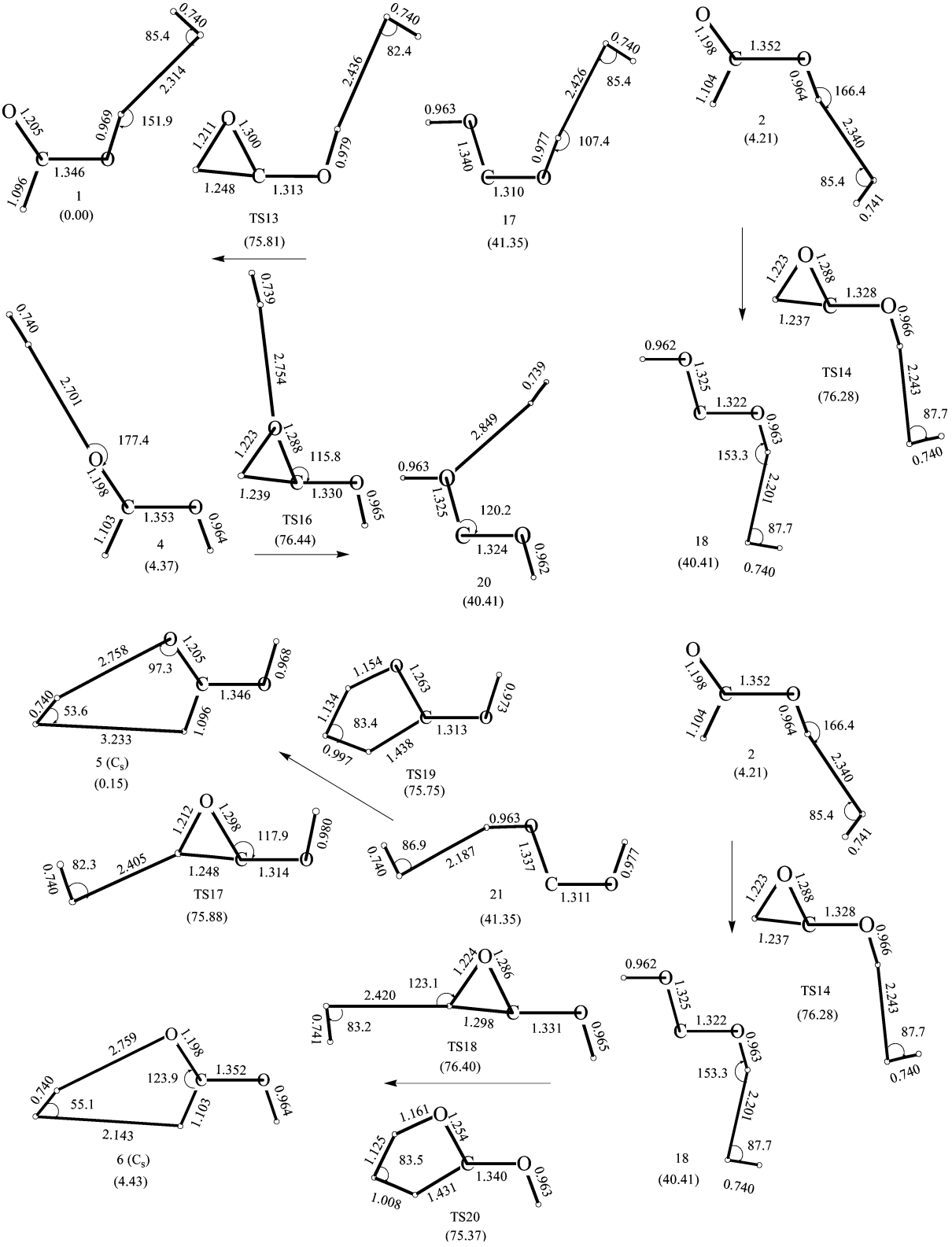

Figure 4. Species involved in formation of $C(OH)_2-H_2$ from $HCOOH-H_2$; bond lengths are in Å; angles are in degrees; the species beside the arrows are transition states; in parentheses, the symmetry (except for C_1) and relative energy (in kcal/mol) of each species are indicated.

kcal/mol relative to that of **1**) indicates that H_2 has some inhibiting effect toward formation of CO and H_2O.

For $C(OH)_2$ to dissociate into CO_2 and H_2, two H atoms of both OH groups should orient in the same direction. Such a conformer can be produced via conformational change (Figure 14). In the presence of H_2, the conformational change of $C(OH)_2$ is limited in certain cases. Starting from **17** or **21**, only conformer **22** can be produced via single-bond rotation. From **22** to $H_2-CO_2-H_2$ (**16**), however, the barrier is as high as 141.70 kcal/mol relative to that of **1**. A seven-membered ring structure involving four H atoms may cause the high energy of transition state TS31 (Figure 7). Another conformer, **24**, can lead to **16** via transition state TS32. The barrier is 76.94 kcal/mol relative to that of **1**. However, conformer **24** cannot be produced via single-bond rotation from other conformers, so the probability for its formation is small. As for conformer **25**,

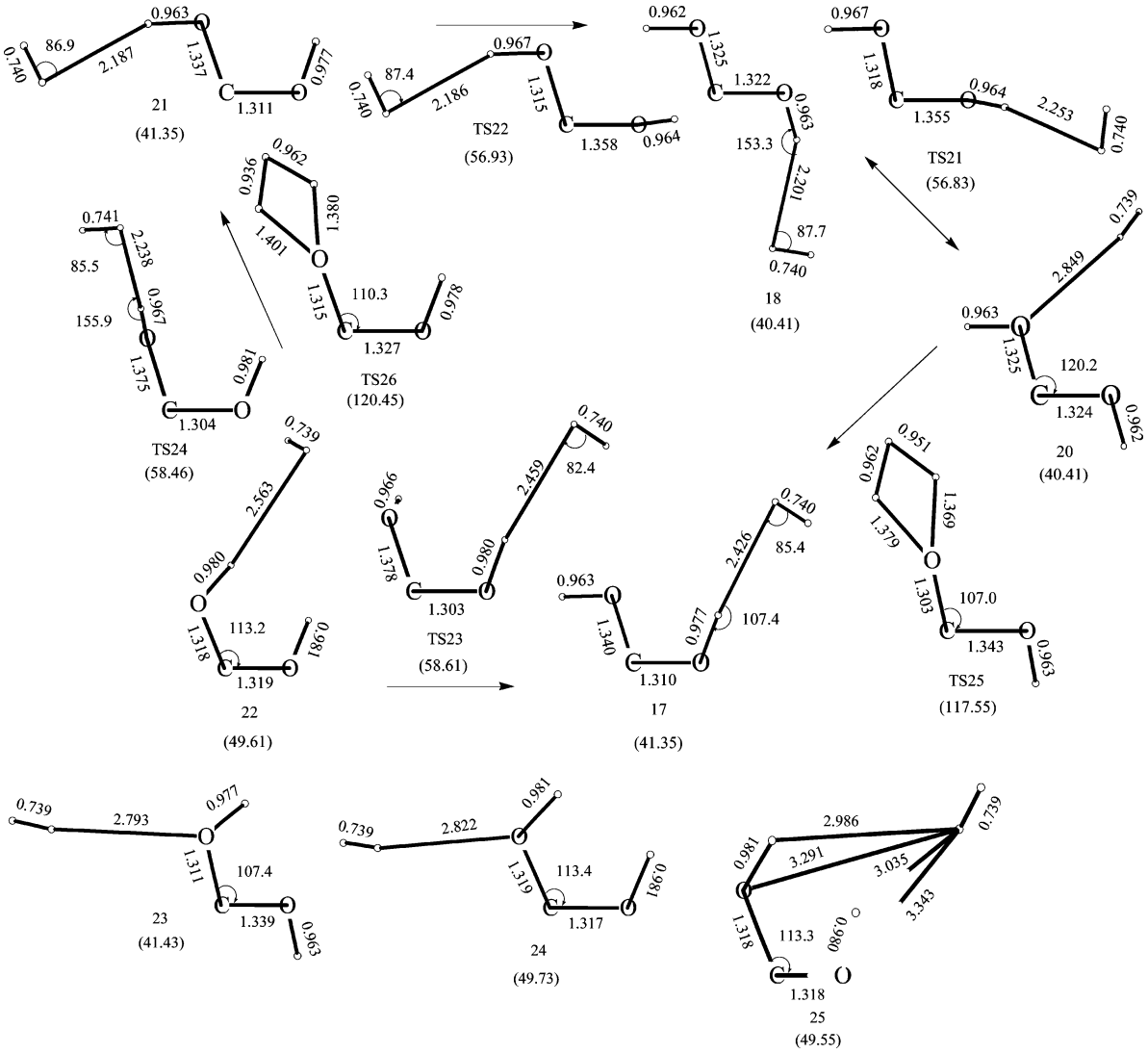

Figure 5. Conformers of $C(OH)_2-H_2$ and transition states of conformational change; bond lengths are in Å; angles are in degrees; the species beside the arrows are transition states; in parentheses, the symmetry (except for C_1) and relative energy (in kcal/mol) of each species are indicated.

no transition states connecting it with **16** are found. Therefore, decomposition of $HCOOH-H_2$ via formation of $C(OH)_2-H_2$ is more likely to result in $CO-H_2O-H_2$ rather than $H_2-CO_2-H_2$.

III.D. Pathways via Formation of $HCHO-H_2O$. Starting from **10**, the weakly bonded H_2 can add to HCOOH via transition state TS33 (Figure 8). H_2 addition accompanies H_2O elimination, resulting in $HCHO-H_2O$ (**29**), a hydrogen-bonded complex of formaldehyde and H_2O. The barrier for this process is 74.17 kcal/mol relative to that of **1**, energetically competitive with other reaction channels. Starting from **8** with higher energy (100.42 kcal/mol), H_2 addition and H_2O elimination can proceed via a channel involving an H radical (TS34), resulting in $HCOH-H_2O$ (**30**), a complex of *trans*-HCOH and H_2O.

For free HCHO dissociating into CO and H_2, the transition state and barrier height have been well established.[17] As H_2O and HCHO form a relatively stable complex, **29**, dissociating into $CO-H_2O-H_2$ can proceed in several ways (Figure 9). First, H_2 can eliminate from HCHO (TS35 and TS36), resulting in $CO-H_2O-H_2$ (**14**). The energy of TS36 (81.71 kcal/mol relative to that of **1**) is higher than that of TS35 and close to that of dissociation of free HCHO,[17] probably because H_2O involvement in the structure of TS35 lowers the energy barrier. Second, H_2 elimination from **29** can also proceed via multistep pathways. Starting from **29**, H can transfer from C to O, resulting in **30**. Two transition states were located for this conversion. It can be seen that H_2O takes part in the formation of TS37 but is less involved in TS38. As a result, the energy of TS37 (58.41 kcal/mol relative to that of **1**) is much lower than that of TS38 (83.58 kcal/mol relative to that of **1**). In **30**, H_2O acts as a strong hydrogen-bonding acceptor as well as a weak donor. In another complex $HCOH-H_2O$ (**31**), H_2O acts purely as a hydrogen-bonding donor. As a result, the energy of **31** (55.79 kcal/mol) is higher than that of **30** (48.68 kcal/mol). Also starting from **29**, H transfer from carbon to oxygen can proceed via transition state TS39, resulting in **31**. Because H_2O is essentially not involved in TS39, the barrier is higher (86.19 kcal/mol relative to that of **1**).

To be feasible for H_2 elimination, the *trans*-HCOH in **30** or **31** needs to convert to the cis one as in $HCOH-H_2O$ (**32**) and $HCOH-H_2O$ (**34**). The energy of **32** is 55.01 kcal/mol relative to that of **1**. Its formation from **30** can be realized via single-bond rotation as shown by transition state TS40. The barrier is 77.35 kcal/mol relative to that of **1**. The reaction channel from **31** to **32**, via H_2O involved H transfer (TS41), requires 100.81kcal/mol energy for the system. H_2 elimination from **32** results in $CO-H_2O-H_2$ (**26**). There are three possible channels leading **32** to **26** or **14**. The channel with lowest energy is via a six-membered ring structured transition state TS42. This is a H_2O-catalyzed process with a barrier of 77.82 kcal/mol relative

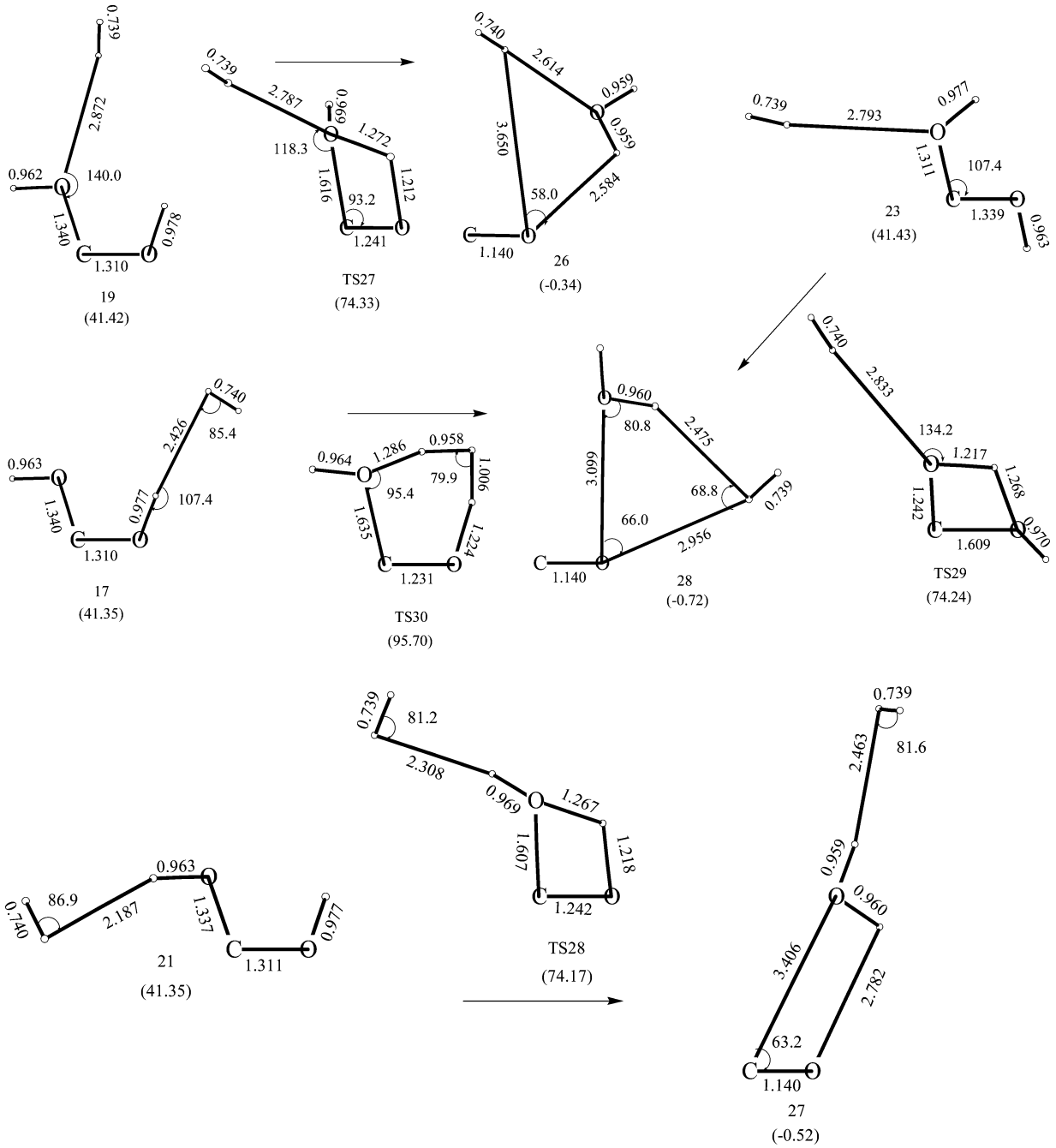

Figure 6. Species involved in pathways from $C(OH)_2-H_2$ to $CO-H_2O-H_2$; bond lengths are in Å; angles are in degrees; the species beside the arrows are transition states; in parentheses, the symmetry (except for C_1) and relative energy (in kcal/mol) of each species are indicated.

to that of **1**. In transition state TS43, H_2 elimination is via a four-membered ring structure, seemingly not helped by H_2O. In TS44, a six-membered ring structure is similar to that of TS42, but the position of carbon is exchanged with that of oxygen, thus raising the energy of the transition state. Consequently, the energies of TS43 and TS44 are 100.65 and 106.57 kcal/mol relative to that of **1**.

It is clear that formation of HCHO or HCOH, followed by H_2O-catalyzed H_2 elimination will produce CO. Conditions that favor H_2 addition to HCOOH may raise the CO/CO_2 ratio.

III.E. Pathways via Formation of $CH_2(OH)_2$. Starting from **5** or **6**, H_2 adds to HCOOH via transition state TS45 or TS46, resulting in methanediol $CH_2(OH)_2$ (**33**) (Figure 10). The barrier of this process is 78.80 or 83.74 kcal/mol relative to that of **1**, higher but still comparable with those of the other reaction channels. $CH_2(OH)_2$ can be in three conformers due to relative orientations of its OH groups. Only **33**, with the lowest energy, is shown because the other two conformers are energetically close to **33**, and the barriers of interconversion between them, via single O−H bond rotation, are very small.

Upon formation, $CH_2(OH)_2$ is quite easy to dehydrate into HCHO (Figure 11). H_2O forms via H transfer between two OH groups of **33** (TS47), resulting in **29**. The barrier is 46.41 kcal/mol relative to that of **1**. This is a well-studied process. The geometry structure and barrier height calculated in this work are very close to those reported by others.[18] Starting from **33**, the other two dehydration channels require energies of 71.49 and 72.89 kcal/mol relative to that of **1**. H_2O forms via H transfer from carbon to an OH group (TS48 or TS49), resulting in **30** or $HCOH-H_2O$ (**34**), a loose association of *cis*-HCOH and H_2O. Without H_2O's help, H_2 eliminating from **34** requires quite high energy of 108.03 kcal/mol (TS50) (Figure 9). The

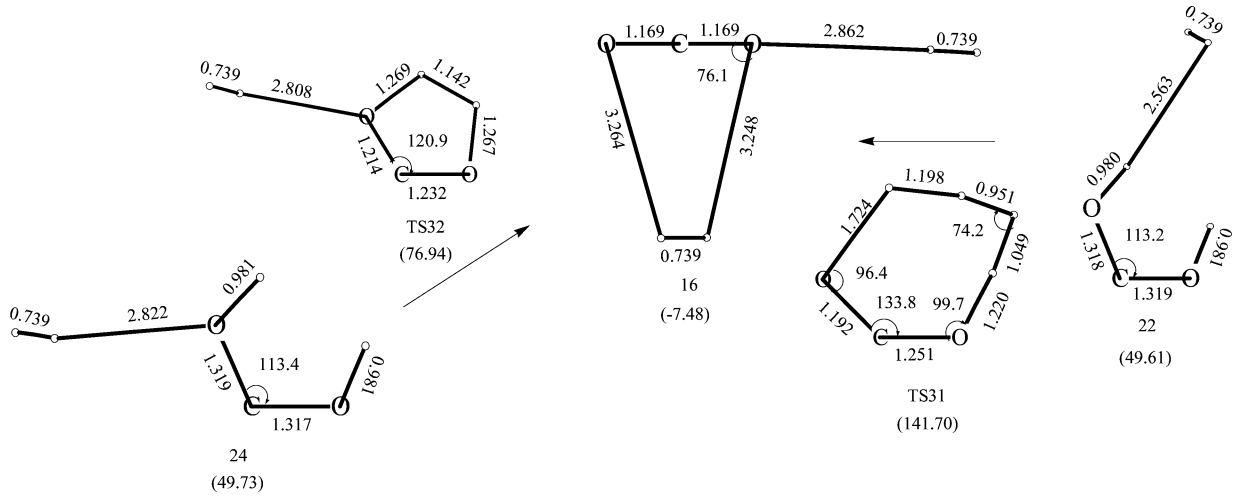

Figure 7. Species involved in pathways from $C(OH)_2-H_2$ to $H_2-CO_2-H_2$; bond lengths are in Å; angles are in degrees; the species beside the arrows are transition states; in parentheses, the symmetry (except for C_1) and relative energy (in kcal/mol) of each species are indicated.

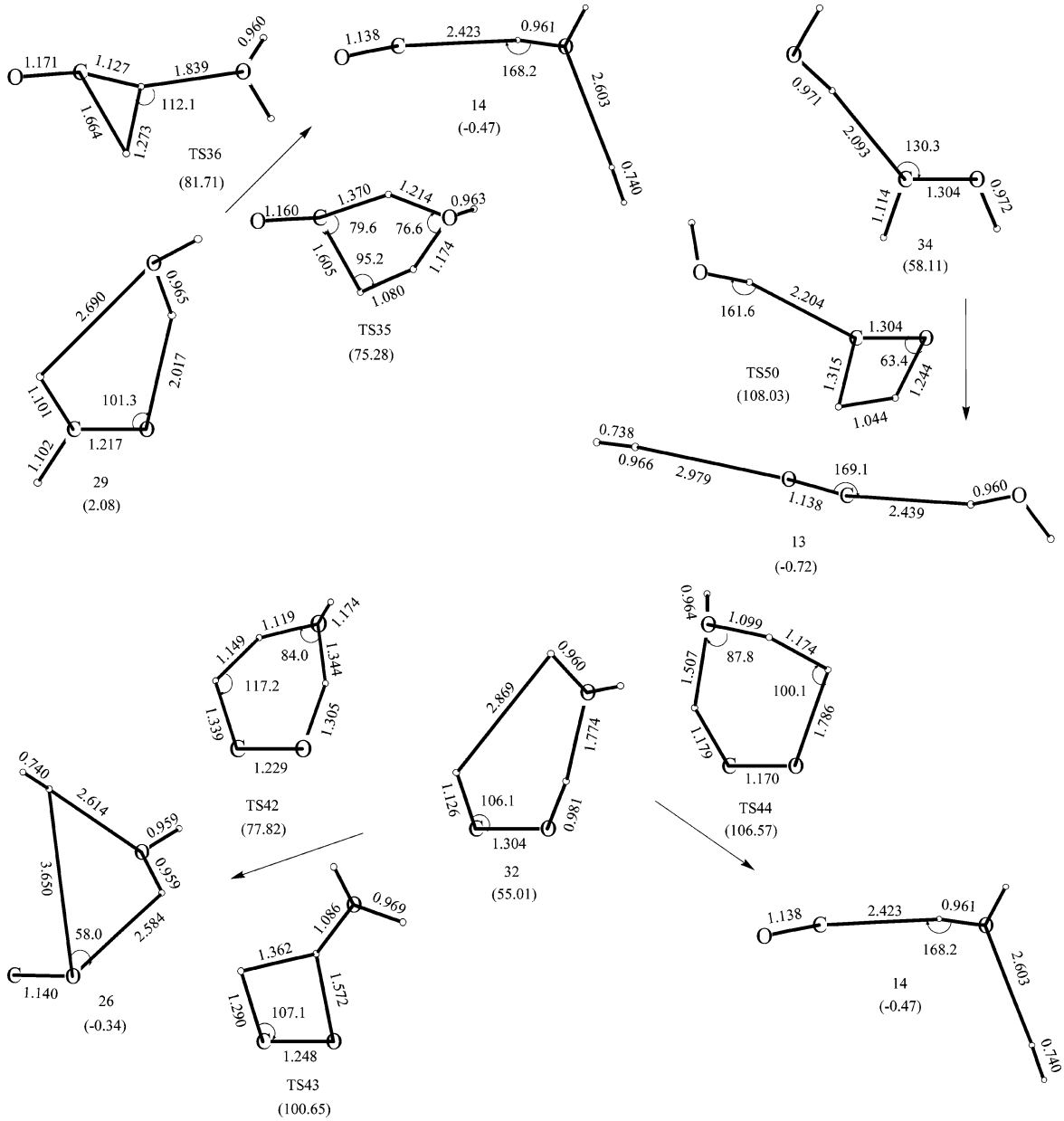

Figure 8. Species involved in pathways from $HCOOH-H_2$ to $HCHO-H_2O$ and $HCOH-H_2O$; bond lengths are in Å; angles are in degrees; the species beside the arrows are transition states; in parentheses, the symmetry (except for C_1) and relative energy (in kcal/mol) of each species are indicated.

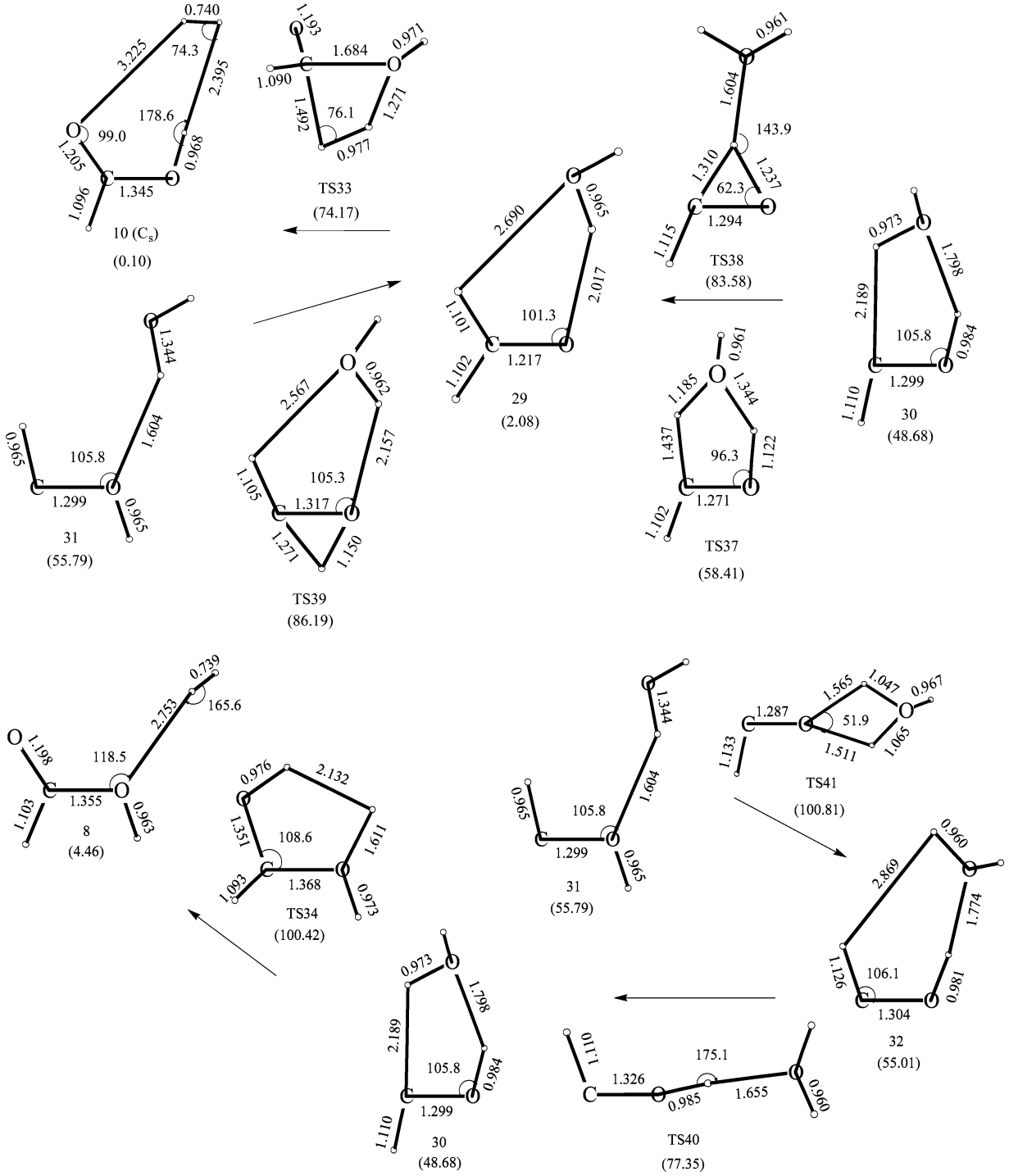

Figure 9. Species involved in pathways from HCHO−H_2O and HCOH−H_2O to CO−H_2O−H_2; bond lengths are in Å; angles are in degrees; in parentheses, the symmetry (except for C_1) and relative energy (in kcal/mol) of each species are indicated.

product is CO−H_2O−H_2 (**14**). Nevertheless, as described in section III.D., because both HCHO and HCOH are subject to further dissociation in the presence of H_2O, $CH_2(OH)_2$ can be seen as a intermediate connecting HCOOH−H_2 and CO−H_2O−H_2.

Raising the energies to the system to a higher level, $CH_2(OH)_2$ is able to eliminate H_2 in other ways (Figure 12). Two H atoms of the CH_2 group in $CH_2(OH)_2$ associate into H_2, which then eliminates (TS51, TS52, and TS53), resulting in $C(OH)_2$−H_2 **21**, **18**, and **25**. The barriers for these processes are 83.20, 84.29, and 88.24 kcal/mol relative to that of **1**, indicating that such channels are not energetically favored.

Therefore, pathways via formation of $CH_2(OH)_2$ lead most probably to dehydration and result in CO−H_2O−H_2 as the final product.

IV. Conclusion

The H_2 molecule, produced by decarboxylation of HCOOH, influences further decomposition of HCOOH in several ways. As shown in Figure 14, for free HCOOH, the decomposition channels leading to CO + H_2O are competitive with those leading to CO_2 + H_2. When HCOOH weakly bonds to H_2, the cis−trans conversion is somewhat hindered. Because *cis*-HCOOH is less populated than the trans one, upon activation,

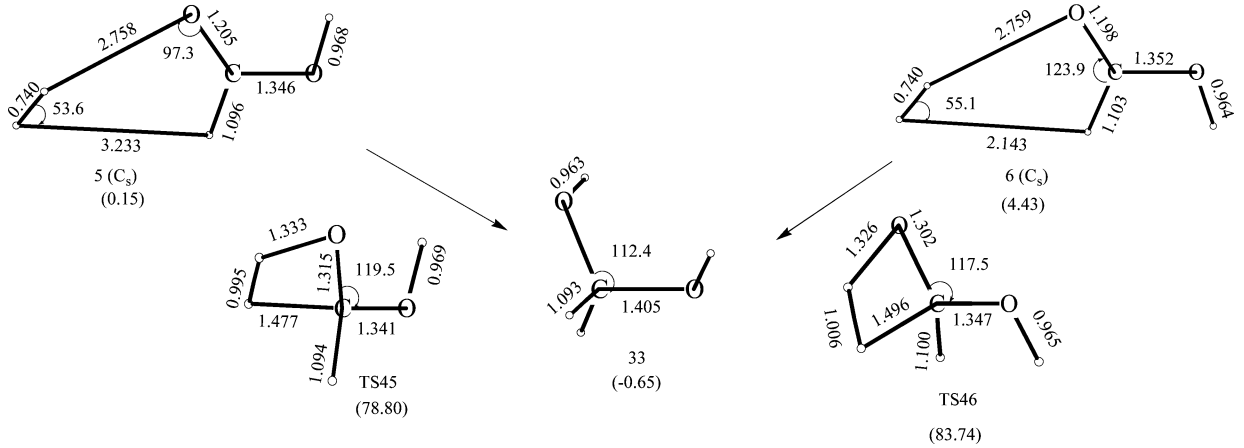

Figure 10. Species involved in pathways from $HCOOH-H_2$ to $CH_2(OH)_2$; bond lengths are in Å; angles are in degrees; the species beside the arrows are transition states; in parentheses, the symmetry (except for C_1) and relative energy (in kcal/mol) of each species are indicated.

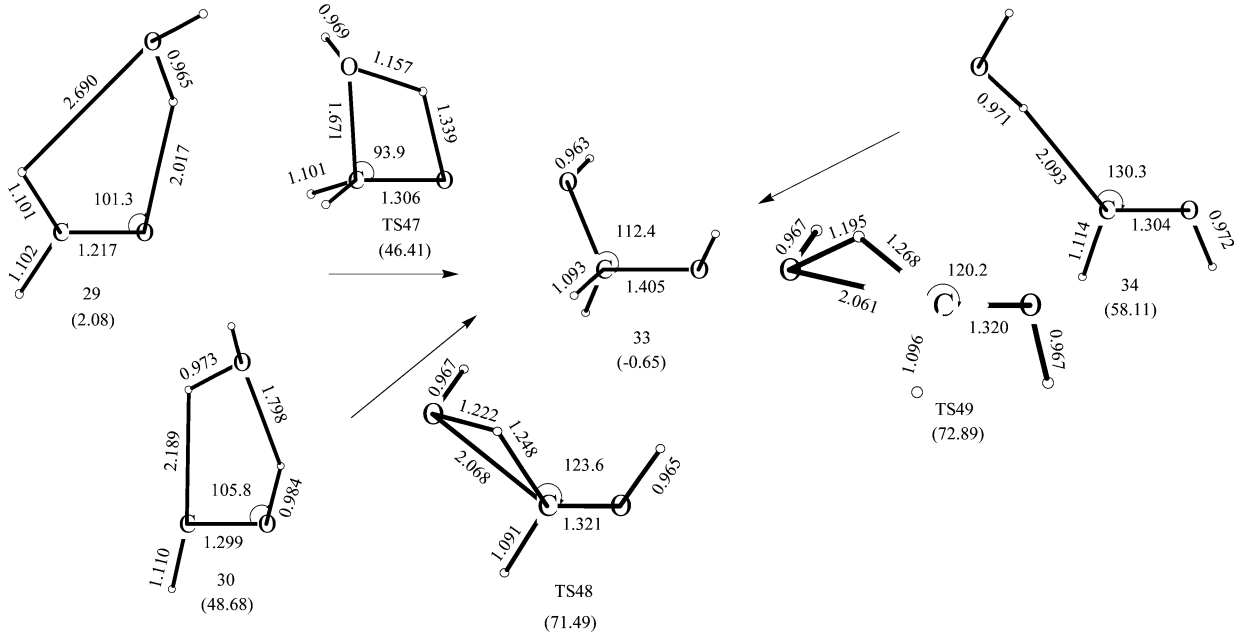

Figure 11. Species involved in pathways from $CH_2(OH)_2$ to $HCHO-H_2O$ and $HCOH-H_2O$; bond lengths are in Å; angles are in degrees; the species beside the arrows are transition states; in parentheses, the symmetry (except for C_1) and relative energy (in kcal/mol) of each species are indicated.

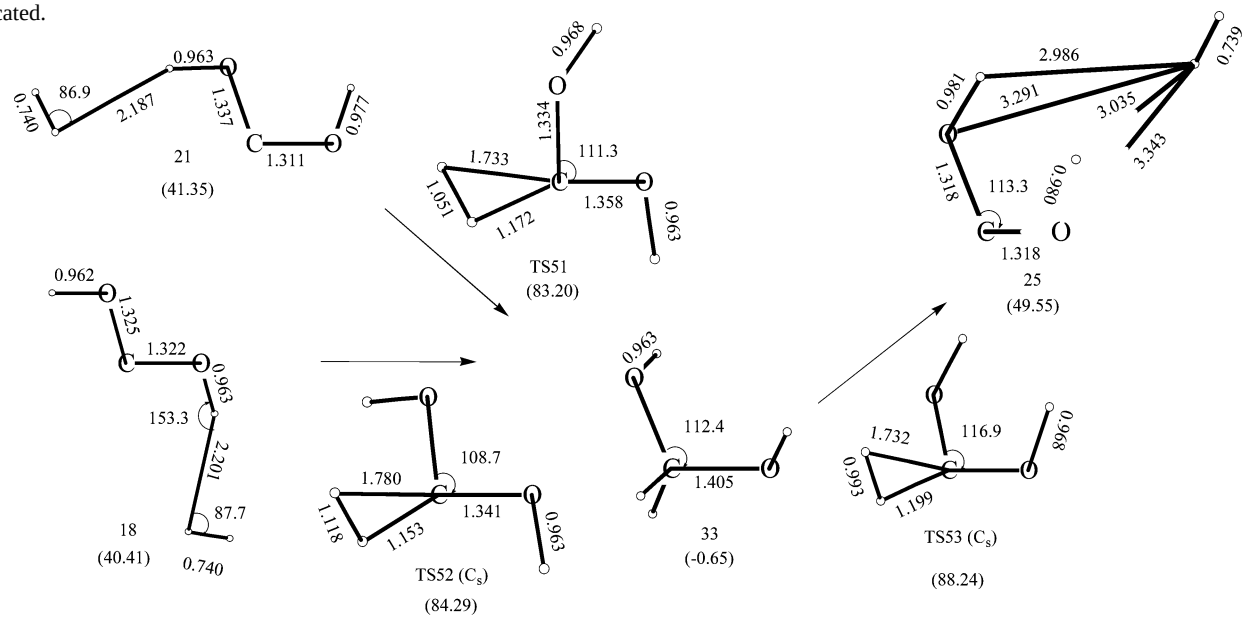

Figure 12. Species involved in pathways from $CH_2(OH)_2$ to $C(OH)_2-H_2$; bond lengths are in Å; angles are in degrees; the species beside the arrows are transition states; in parentheses, the symmetry (except for C_1) and relative energy (in kcal/mol) of each species are indicated.

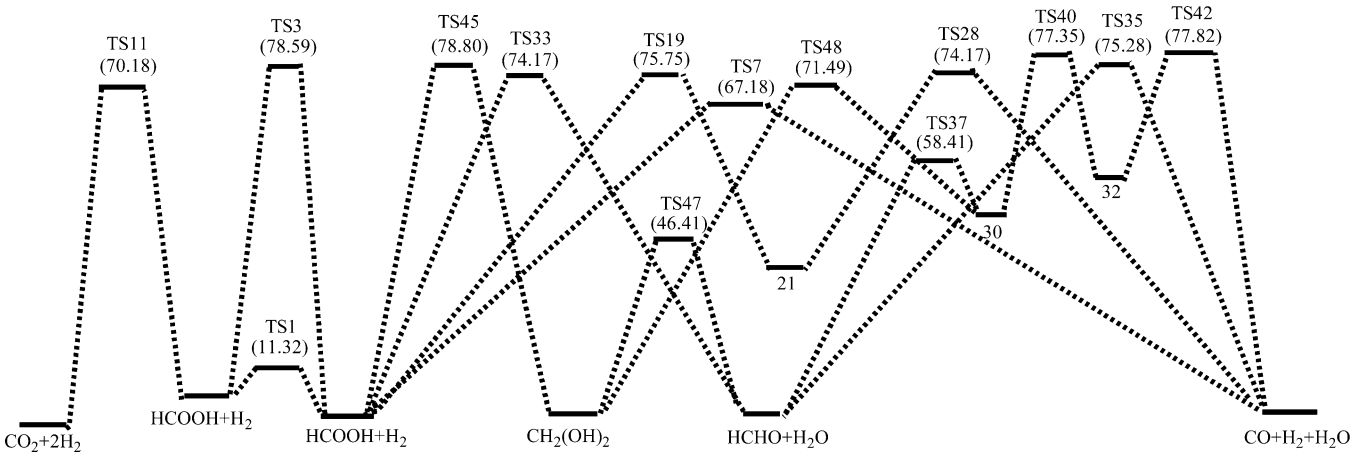

Figure 13. Decomposition pathways of HCOOH + H_2 with energies less than 80 kcal/mol relative to that of HCOOH−H_2 (**1**). Relative energies are values calculated at the CCSD(T)/6-311++G**//MP2/6-311++G** level with ZPE correction.

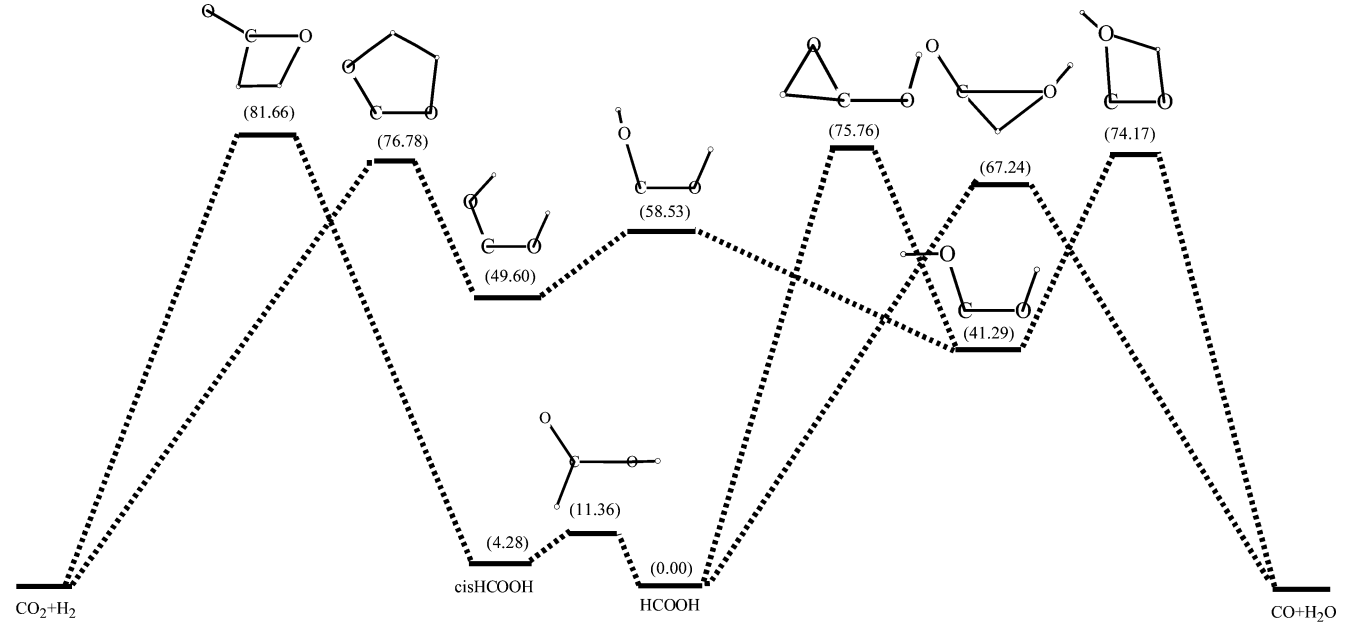

Figure 14. Decomposition pathways of free HCOOH. Relative energies (in kcal/mol), shown in parentheses, are values calculated at the CCSD-(T)/6-311++G**//MP2/6-311++G** level with ZPE correction (ref 15).

the probability of dehydration to CO + H_2O is larger than that of decarboxylation to CO_2 + H_2. Furthermore, in the presence of H_2, the reaction channel leading to CO via intermediate $C(OH)_2$ is not influenced essentially, whereas the channel leading to CO_2 is hindered because the *cis*-$C(OH)_2$ conformer required for H_2 elimination is difficult to form. More importantly, under competitive energetic conditions, H_2 can add to HCOOH, resulting in HCHO and H_2O, or $CH_2(OH)_2$ followed by dissociating into HCHO and H_2O. With H_2O as a catalyst, HCHO can further dissociate into CO and H_2. As summarized in Figure 13, with energy less than 80 kcal/mol, decomposition of HCOOH−H_2 can lead to CO + H_2O + H_2 via several reaction channels, statistically more favored than that leading to CO_2 + $2H_2$ via a single-reaction channel. Consequently, H_2 accumulation during decomposition of HCOOH is probably the major reason that accounts for the large CO/CO_2 ratio indicated by some experiments. In some cases, chemical bonding like H−H−H and H−H−H−H, appearing in certain transition states, is responsible for the high energetic barriers. To reveal the nature of such bonding types, further investigation is necessary.

Supporting Information Available: Table showing the electronic energies, dipole moments, and rotational constants of the species in the decomposition of HCOOH−H_2. This material is available free of charge via the Internet at http://pubs.acs.org.

References and Notes

(1) Blake, P. G.; Davies, H. H.; Jackson, G. E. *J. Chem. Soc. B* **1971**, 1923.

(2) Hsu, D. S. Y.; Shaub, W. M.; Blackbum, M.; Lin, M. C. Proceedings of the 19th International Symposium on Combustion; The Combustion Institute: Pittsburgh, PA, 1983.

(3) Saito, K.; Kakamoto, T.; Kuroda, H.; Torii, S.; Imamura, A. *J. Chem. Phys.* **1984**, *80*, 4989.

(4) Goddard, J. D.; Yamaguchi, Y.; Schaefer, H. F. *J. Chem. Phys.* **1992**, *96*, 1158.

(5) Francisco, J. S. *J. Chem. Phys.* **1992**, *96*, 1167.

(6) Ruelle, P.; Kesselring, U. W.; Nam-tran, H. *J. Am. Chem. Soc.* **1986**, *108*, 371.

(7) Tokmakov, I. V.; Hsu, C. C.; Moskaleva, L. V.; Lin, M. C. *Mol. Phys.* **1997**, *92*, 581.

(8) Wang, B. S.; Hou, H.; Gu, Y. S. *J. Phys. Chem. A* **2000**, *104*, 10526.

(9) Yagasaki, T.; Saito, S.; Ohmine, I. *J. Chem. Phys.* **2002**, *117*, 7631.

(10) Koryabkina, N. A.; Phatak, A. A.; Ruettinger, W. F.; Farrauto, R. J.; Ribeiro, F. H. *J. Catal.* **2003**, *217*, 233.

(11) Henderson, M. A. *J. Phys. Chem. B* **1997**, *101*, 221.

(12) Rasko, J.; Kecskes, T.; Kiss, J. *J. Catal.* **2004**, *224*, 261.

(13) Peng, C. Y.; Ayala, P. Y.; Schlegel, H. B.; Frisch, M. J. *J. Comput. Chem.* **1996**, *17*, 49.

(14) Frisch, M. J.; Trucks, G. W.; Schlegel, H. B.; Scuseria, G. E.; Robb, M. A.; Cheeseman, J. R.; Zakrzewski, V. G.; Montgomery, J. A., Jr.; Stratmann, R. E.; Burant, J. C.; Dapprich, S.; Millam, J. M.; Daniels, A. D.; Kudin, K. N.; Strain, M. C.; Farkas, O.; Tomasi, J.; Barone, V.; Cossi, M.; Cammi, R.; Mennucci, B.; Pomelli, C.; Adamo, C.; Clifford, S.; Ochterski, J.; Petersson, G. A.; Ayala, P. Y.; Cui, Q.; Morokuma, K.; Malick, D. K.; Rabuck, A. D.; Raghavachari, K.; Foresman, J. B.; Cioslowski, J.; Ortiz, J. V.; Stefanov, B. B.; Liu, G.; Liashenko, A.; Piskorz, P.; Komaromi, I.; Gomperts, R.; Martin, R. L.; Fox, D. J.; Keith, T.; Al-Laham, M. A.; Peng, C. Y.; Nanayakkara, A.; Gonzalez, C.; Challacombe, M.; Gill, P. M. W.; Johnson, B. G.; Chen, W.; Wong, M. W.; Andres, J. L.; Head-Gordon, M.; Replogle, E. S.; Pople, J. A. *Gaussian 98*, revision A.7; Gaussian, Inc.: Pittsburgh, PA, 1998.

(15) Hu, S. W.; Lu, S. M.; Wang, X. Y. *J. Phys. Chem. A* **2004**, *108*, 8485.

(16) The value is calculated using the same method as the other species.

(17) Scuseria, G. E.; Schaefer, H. F. *J. Chem. Phys.* **1989**, *90*, 3629.

(18) Kent, D. R.; Widicus, S. L.; Blake, G. A.; Goddard, W. A. *J. Chem. Phys.* **2003**, *119*, 5117.